Poration of lipid bilayers by shock-induced nanobubble collapse

Amit Choubey, Mohammad Vedadi, Ken-ichi Nomura, Rajiv K. Kalia,[a] Aiichiro Nakano, and Priya Vashishta[a]

Collaboratory for Advanced Computing and Simulations, Department of Physics and Astronomy, Department of Chemical Engineering and Materials Science, and Department of Computer Science, University of Southern California, Los Angeles, California 90089-0242, USA

(Received 9 July 2010; accepted 19 October 2010; published online 10 January 2011)

We investigate molecular mechanisms of poration in lipid bilayers due to shock-induced collapse of nanobubbles. Our multimillion-atom molecular dynamics simulations reveal dynamics of nanobubble shrinkage and collapse, leading to the formation and penetration of nanojets into lipid bilayers. The nanojet impact generates shear flow of water on bilayer leaflets and pressure gradients across them, which transiently enhance the bilayer permeability by creating nanopores through which water molecules translocate rapidly across the bilayer. Effects of nanobubble size and temperature on the porosity of lipid bilayers are examined. © *2011 American Institute of Physics*. [doi:10.1063/1.3518472]

In recent years, noninvasive drug- and gene-delivery approaches have garnered significant interest because of direct applications in cancer treatment and gene therapy. Much of the experimental effort is focused on designing a targeted approach that has both spatial and temporal specificities. Research in this area relies mainly on the use of electric fields or pressure waves to enhance the permeability of cell membranes. In one of the most commonly used techniques known as electroporation,[1] electric fields are applied across the cell to increase the cell-membrane permeability. Reversible electroporation, in which the cell permeability is enhanced temporarily, is used for drug delivery and gene therapy. Electric fields applied over a sufficiently long time can kill the cell because of temperature elevation resulting from Joule heating. This irreversible electroporation process is commonly used in the food industry to inactivate microbes and also in minimally invasive treatment of cancerous tissues.

Sonoporation is another promising DNA-, protein-, and drug-delivery approach.[2] To achieve high efficiency in sonoporation, *in vivo* gas bubbles are used in conjunction with diagnostic level ultrasound exposures.[3] Sonoporation experiments show that the collapse of bubbles by ultrasound generates water jets[4] whose impact on the cell membrane increases the permeability, thereby allowing the intracellular delivery of drug/gene payload.[5] Shock waves in tandem with nanobubbles provide another promising approach to targeted delivery of drugs and genes. Shock-wave phenomena,[6] such as extracorporeal shock-wave lithotripsy, have been used in living tissues.

The present work focuses on poration of lipid bilayers by the interaction of shock waves with nanobubbles. We have performed molecular dynamics (MD) simulations to study the impact of shock waves on nanobubbles in the vicinity of a dipalmitoylphosphatidylcholine (DPPC) phospholipid bilayer embedded in water. We use GROMACS (Ref. 7) to simulate the simple point charge (SPC) model for water[8] and DPPC bilayer. In our MD simulations, a nanobubble is created close to the lipid bilayer by removing water molecules within a sphere of diameter D. The simulations were done for $D=10,20,40$ nm, and these systems contain about 1.9×10^6, 6.2×10^6, and 30.8×10^6 atoms, respectively; the dimensions of the corresponding MD cells are $19\times19\times61$, $34\times34\times82$, and $64\times64\times92$ nm^3. The parameters for bonded and nonbonded interactions as well as partial charges on atoms in the DPPC bilayer system are taken from Refs. 9 and 10. The force field for DPPC molecule is validated against experimental data for area per lipid and order parameter.[9,11] Bending modulus and gel to liquid-crystalline phase transition temperature obtained from MD simulation are also in good agreement with experiments.[12] The lateral diffusion coefficient for DPPC molecules in bilayers has been measured experimentally.[13] In the fluid phase the value ranges between 0.6×10^{-7} and 2×10^{-7} cm^2/s, whereas in the gel phase it ranges between 0.04×10^{-9} and 16×10^{-9} cm^2/s. In coarse-grained MD simulations based on all-atom MD simulation described here, the lateral diffusion coefficient is between 1×10^{-7} and 4×10^{-7} cm^2/s in the fluid phase and between 0.5×10^{-9} and 4×10^{-9} cm^2/s in the gel phase.[14]

We checked the validity of the SPC model for water under shock.[15] First we equilibrated the system for 1 ns using a time step of 2 fs. To apply shock, we inserted a vacuum layer of thickness equal to 2 nm at the end of the MD box in the x direction and moved the system with a constant particle velocity u_p toward a momentum mirror,[16] i.e., along $-x$ in the inset of Fig. 1. The mirror reverses the x-component of atomic velocity if an atom crosses the mirror plane. This generates a planar shock in the $+x$ direction. The shock velocity u_s is determined by monitoring the shock front, i.e., discontinuity in pressure or mass density of water at two instants of time. Figure 1 shows that the MD results for u_s as a function of u_p are in good agreement with experimental data.[17]

Next, we performed MD simulations to equilibrate initial configurations of lipid bilayers and water molecules at temperatures $T_i=300$ and 323 K and pressure $P=1$ bar using a time step of 2 fs. After equilibration we created a bubble near the bilayer (see Fig. S1 in the supplementary material[18]) and applied planar shock as discussed above. A number of simulations were performed for different nanobubble diameters

[a]Authors to whom correspondence should be addressed. Electronic addresses: rkalia@usc.edu and priyav@usc.edu.

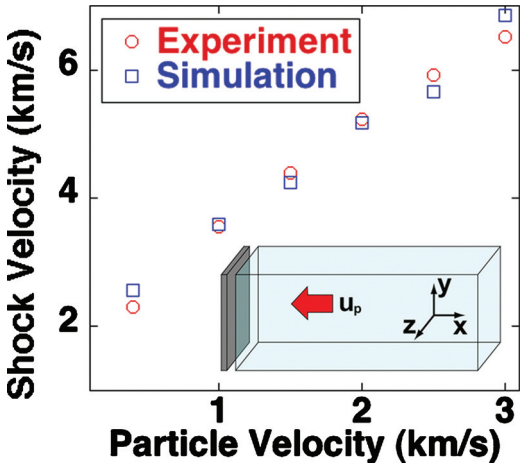

FIG. 1. (Color) Shock velocity vs particle velocity. The simulation results for SPC water are in good agreement with experimental data. The inset shows the setup for shock simulation. The gray plate is the momentum mirror.

(D=10, 20, and 40 nm), particle velocities (u_p=0.4, 0.7, and 1 km/s), and initial temperatures (T_i=300 and 323 K).

When a planar shock front hits the proximal side of a nanobubble, water molecules from the bubble periphery accelerate toward the center of the bubble and form a nanojet. The size of the nanojet depends on the particle velocity and nanobubble diameter. As the particle velocity increases from 0.4 to 1.0 km/s, the number of water molecules in the nanojet for a fixed value of D increases by an order of magnitude. Figure 2 displays instantaneous molecular velocities averaged in voxels of dimension 0.5 nm for a bubble of initial diameter D=40 nm under the impact of a shock front moving with velocity u_p=0.7 km/s. Figure 2(a) shows that velocities of water molecules in the domain of the shrinking nanobubble are focused in the form of a nanojet. As the particle velocity increases from 0.4 to 1.0 km/s, the average x-component of molecular velocities inside the nanojet increases from 2.6 to 3.5 km/s for all simulated nanobubble sizes. For D=40 nm, we find that the length of the nanojet l_{jet} is 57 nm. Our results for other nanobubble sizes and particle velocities also indicate that the length of the jet scales as $l_{jet} \approx 1.5D$. Surprisingly, the same linear scaling has been observed in experimental studies of shock-induced collapse of micron-to-millimeter size bubbles.[4,19]

We have performed additional simulations of nanobubble collapse in water at a particle velocity of 3 km/s. We find the bubble collapse times to be 0.9, 1.2, and 1.5 ps for bubble diameters of 6, 8, and 10 nm, respectively. Using the Rayleigh formula ($\tau = 0.45D\sqrt{\rho/\Delta P}$, where ρ is the mass density and ΔP is the pressure difference across the bubble surface), we obtain τ to be 0.8, 1.1, and 1.3 ps for the three bubble sizes. The differences between our calculation and the estimates from the Rayleigh formula arise from the facts that (1) in Rayleigh collapse it is assumed that the bubble collapses within a fluid of uniform pressure and density, whereas in our simulations pressure and density become nonuniform due to the shock front; and (2) the Rayleigh equation does not include viscosity and surface tension effects which arise due to interatomic interactions. From the onset of nanojet formation and disintegration, we have determined that the persistence time τ_{jet} for the jet exceeds the bubble collapse time by at least 0.2 ps.

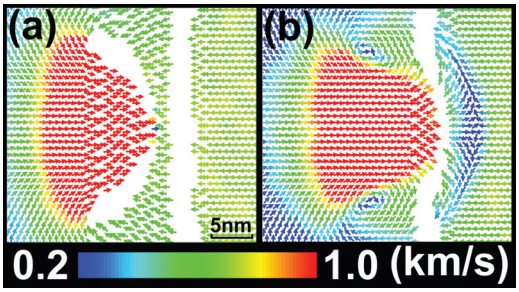

FIG. 2. (Color) Snapshots of velocity profile for the system with D=40 nm, T_i=300 K, and u_p=0.7 km/s. Arrows show the direction of average molecular velocities and the velocity magnitudes are color-coded. (a) shows a nanojet in the system at t=20 ps. The white vertical region is the bilayer. (b) shows a spreading flow at t=24 ps resulting from the impact of the nanojet on the lipid bilayer.

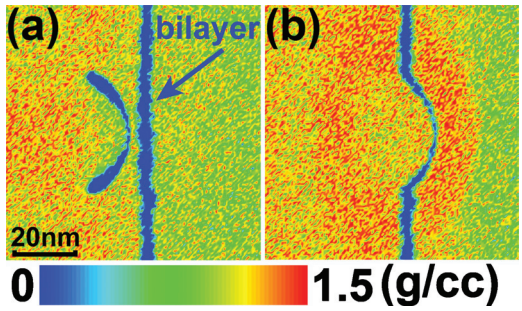

FIG. 3. (Color) (a) and (b) are snapshots of the density of water at t=20 and 28 ps. Here D=40 nm, T_i=300 K, and u_p=0.7 km/s. The central blue region is the lipid bilayer. (a) shows the nanojet traveling toward the distal side of the nanobubble. (b) shows the deformed bilayer and water-hammer shock.

In Fig. 2(b) we show the interaction between water molecules in the nanojet and the DPPC molecules in the bilayer. Water molecules in the nanojet form a spreading flow after hitting the leaflet of the DPPC bilayer (see Fig. S2 in the supplementary material[18]).[5] We also observe vortices in the collapsed bubble when water molecules bouncing back from the bilayer encounter other water molecules in the incoming shock wave.

Figure 3(a) shows the water density around the DPPC bilayer (blue region) just before the bilayer is hit by the water nanojet from a collapsing nanobubble of diameter equal to 40 nm at u_p=0.7 km/s. The curved blue region to the left of the bilayer indicates that the bubble has not collapsed completely, and the water density around the nanobubble is close to the normal density of water. After the nanojet impact, the DPPC bilayer deforms and becomes significantly disordered (see the supplementary material[18]). The water density around the bilayer leaflet closer to the collapsed bubble increases to 1.5 g/cc. Figure 3(b) shows that the deformed bilayer is hemispherical. In addition, we observe water-hammer shock when water molecules in the nanojet hit the distal side of the nanobubble. This secondary water-hammer shock spreads spherically, and its initial speed (until 4 ps after formation) is approximately 1.6 km/s. The amplitude of the secondary shock decreases, but its velocity increases with time. Secondary water-hammer shocks have been observed in experiments[20] and continuum simulations.[21]

The averaged lateral velocity of water molecules in the vicinity of a lipid bilayer versus the distance from the center of the bilayer is shown in Fig. S2 (see the supplementary

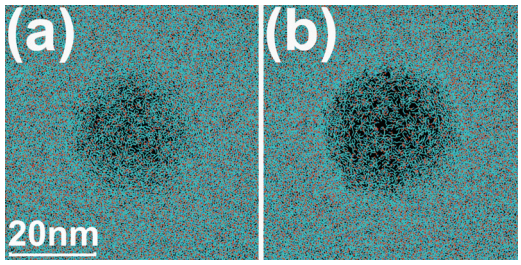

FIG. 4. (Color) Poration of lipid bilayers by collapsed nanobubbles. Here u_p=0.7 km/s and D=40 nm. In (a), the bilayer was initially in the gel phase at T_i=300 K, and in (b) it was in the liquid phase at T_i=323 K.

material[18]). The peak in the lateral-flow velocity appears when the nanojet hits the bilayer. The distance over which the lateral velocity is larger than the thermal velocity is half the nanobubble radius. Experiments[22] on millimeter size bubbles in the vicinity of a hard surface indicate that this distance is of the order of the bubble radius. The differences between experimental and our MD results are due to the fact that bubble sizes differ by several orders of magnitude, and the surfaces are soft in MD simulation and hard in experiments.

The impact of the nanojet causes poration in the lipid bilayer. Figure 4 shows poration resulting from the impact of the collapsed nanobubble of initial diameter equal to 40 nm at u_p=0.7 km/s. The poration was calculated by dividing the impacted region of the bilayer into pixels of size equal to 0.1 nm and determining the area of empty pixels, i.e., those containing no lipid molecules. For the bilayer initially in the gel phase[23] at T_i=300 K, the nanojet impact increases poration by a factor of 30 over its normal value before the nanojet impact; see Fig. 4(a). For the bilayer initially in the liquid phase[23] at T_i=323 K the poration increases by another factor of 5 relative to the poration in the gel phase; see Fig. 4(b). In the liquid phase at 323 K, the maximum nanopore size is 0.7 nm as compared to 0.4 nm in the gel phase. The poration varies with the particle velocity and nanobubble diameter. At u_p=0.4 km/s, we do not observe any significant change in the porosity of the gel phase for the three bubble sizes we have considered. However, at u_p=1 km/s the maximum nanopore size increases to 0.3 nm for D=10 nm, and it increases linearly with the initial diameter of the nanobubble.

In the deformed DPPC bilayer that was initially in the liquid phase, the pores are large enough ($\geq$0.5 nm) to allow rapid translocation of water molecules. Translocation events are observed for u_p=1.0 km/s and $D \geq 10$ nm and also for u_p=0.7 km/s and D=40 nm; see the movie in the supplementary material.[18] Water molecules can diffuse through the lipid bilayer in the absence of shock, but the diffusion is almost four-orders-of-magnitude slower than in bulk water.[24] The poration by nanojet impact and the large pressure difference ($\sim$9 GPa) across the bilayer combine to shorten the average time of passage for water molecules by six orders of magnitude. The bilayer poration is, however, temporary because the nanopores disappear and the bilayer heals after the passage of shock wave (see Fig. S4 in the supplementary material[18]).

In summary, multimillion-atom MD simulations reveal the mechanism of transient poration in lipid bilayers by shock-induced collapse of nanobubbles. When a planar shock front strikes a nanobubble, water molecules from the bubble periphery accelerate toward the center of the bubble to form a nanojet. The length of the nanojet scales linearly with the initial nanobubble size which, surprisingly, is also observed in experimental studies of shock-induced collapse of micron-to-millimeter size bubbles. The MD simulations reveal that the nanojet impact significantly deforms and thins the lipid bilayer and water molecules in the nanojet form a spreading flow pattern after the impact. Deformation and thinning of bilayers combined with large pressure gradients across and spreading flow around the bilayers create transient nanochannels through which water molecules translocate across the bilayer.

We thank Noah Malmstadt for many useful discussions. This work was supported by NSF-PetaApps and NSF-EMT grants.

[1]A. Golberg and B. Rubinsky, Biomed. Eng. Online **9**, 13 (2010); P. T. Vernier, Y. H. Sun, and M. A. Gundersen, BMC Cell Biol. **7**, 37 (2006).
[2]S. Mitragotri, Nat. Rev. Drug Discovery **4**, 255 (2005); I. Rosenthal, J. Z. Sostaric, and P. Riesz, Ultrason. Sonochem. **11**, 349 (2004); C. M. H. Newman and T. Bettinger, Gene Ther. **14**, 465 (2007).
[3]M. Tamagawa, I. Yamanoi, N. Ishimatsu, and S. Suetsugu, *World Congress on Medical Physics and Biomedical Engineering 2006* (2007), Vol. 14, Parts 1–6, p. 3236; N. Kudo, K. Okada, and K. Yamamoto, Biophys. J. **96**, 4866 (2009); Y. Zhou, J. M. Cui, and C. X. Deng, *ibid.* **94**, L51 (2008).
[4]C. D. Ohl and R. Ikink, Phys. Rev. Lett. **90**, 214502 (2003).
[5]C. D. Ohl, M. Arora, R. Ikink, N. de Jong, M. Versluis, M. Delius, and D. Lohse, Biophys. J. **91**, 4285 (2006).
[6]A. G. Doukas and N. Kollias, Adv. Drug Delivery Rev. **56**, 559 (2004).
[7]B. Hess, C. Kutzner, D. van der Spoel, and E. Lindahl, J. Chem. Theory Comput. **4**, 435 (2008).
[8]C. D. Berweger, W. F. Vangunsteren, and F. Mullerplathe, Chem. Phys. Lett. **232**, 429 (1995); H. J. C. Berendsen, J. P. M. Postma, W. F. van Gunsteren, and J. Hermans, in *Intermolecular Forces*, Proc. 14th Jerusalem Symposium on Quantum Chemistry and Biochemistry, Jerusalem, Israel, 13–16 April, 1981, edited by A. Pullman (Sprinter, New York, 1981).
[9]D. P. Tieleman and H. J. C. Berendsen, J. Chem. Phys. **105**, 4871 (1996).
[10]O. Berger, O. Edholm, and F. Jahnig, Biophys. J. **72**, 2002 (1997).
[11]P. Mark and L. Nilsson, J. Phys. Chem. A **105**, 9954 (2001).
[12]E. Lindahl and O. Edholm, Biophys. J. **79**, 426 (2000); S. Leekumjorn and A. K. Sum, Biochim. Biophys. Acta **1768**, 354 (2007).
[13]A. L. Kuo and C. G. Wade, Biochemistry **18**, 2300 (1979); B. S. Lee, S. A. Mabry, A. Jonas, and J. Jonas, Chem. Phys. Lipids **78**, 103 (1995).
[14]S. J. Marrink, J. Risselada, and A. E. Mark, Chem. Phys. Lipids **135**, 223 (2005).
[15]We have checked the validity of the SPC model by performing MD simulations for shock-induced nanobubble collapse in water using a reactive force field, which can accurately describe bond breaking/formation and chemical reactions in the system.
[16]K. I. Nomura, R. K. Kalia, A. Nakano, P. Vashishta, A. C. T. van Duin, and W. A. Goddard, Phys. Rev. Lett. **99**, 148303 (2007).
[17]A. P. Rybakov and I. A. Rybakov, Eur. J. Mech. B/Fluids **14**, 323 (1995).
[18]See supplementary material at http://dx.doi.org/10.1063/1.3518472 for methodology and results on lateral velocity, order parameter and healing of the bilayer after shock.
[19]T. Kodama and Y. Tomita, Appl. Phys. B: Lasers Opt. **70**, 139 (2000).
[20]E. A. Brujan, G. S. Keen, A. Vogel, and J. R. Blake, Phys. Fluids **14**, 85 (2002).
[21]E. Johnsen and T. Colonius, J. Acoust. Soc. Am. **124**, 2011 (2008).
[22]C. D. Ohl, M. Arora, R. Dijkink, V. Janve, and D. Lohse, Appl. Phys. Lett. **89**, 074102 (2006).
[23]N. Albon and J. M. Sturtevant, Proc. Natl. Acad. Sci. U.S.A. **75**, 2258 (1978).
[24]A. M. Khakimov, M. A. Rudakova, M. M. Doroginitskii, and A. V. Filippov, Biophysics (Engl. Transl.) **53**, 147 (2008).